Histochem Cell Biol (2017) 147:83–95
DOI 10.1007/s00418-016-1485-9

ORIGINAL PAPER

Encapsulation of human elastic cartilage-derived chondrocytes in nanostructured fibrin-agarose hydrogels

Laura García-Martínez[1,2] · Fernando Campos[1] · Carlos Godoy-Guzmán[1,3] · María del Carmen Sánchez-Quevedo[1] · Ingrid Garzón[1] · Miguel Alaminos[1] · Antonio Campos[1] · Víctor Carriel[1]

Accepted: 23 August 2016 / Published online: 1 September 2016

Abstract The generation of elastic cartilage substitutes for clinical use is still a challenge. In this study, we investigated the possibility of encapsulating human elastic cartilage-derived chondrocytes (HECDC) in biodegradable nanostructured fibrin-agarose hydrogels (NFAH). Viable HECDC from passage 2 were encapsulated in NFAH and maintained in culture conditions. Constructs were harvested for histochemical and immunohistochemical analyses after 1, 2, 3, 4 and 5 weeks of development ex vivo. Histological results demonstrated that it is possible to encapsulate HECDC in NFAH, and that HECDC were able to proliferate and form cells clusters expressing S-100 and vimentin. Additionally, histochemical and immunohistochemical analyses of the extracellular matrix (ECM) showed that HECDC synthetized different ECM molecules (type I and II collagen, elastic fibers and proteoglycans) in the NFAH ex vivo. In conclusion, this study suggests that NFAH can be used to generate biodegradable and biologically active constructs for cartilage tissue engineering applications. However, further cell differentiation, biomechanical and in vivo studies are still needed.

✉ Víctor Carriel
vcarriel@ugr.es

[1] Department of Histology, Tissue Engineering Group, Faculty of Medicine, University of Granada and Instituto de Investigación Biosanitaria ibis. GRANADA, Granada, Spain

[2] Doctoral Program in Biomedicine, University of Granada, Granada, Spain

[3] Unit of Histology (CIBAP), School of Medicine, Universidad de Santiago de Chile, (USACH), Santiago, Chile

Keywords Human elastic cartilage-derived chondrocytes · Fibrin-agarose hydrogels · Extracellular matrix · Tissue engineering · Cell-biomaterials interactions · Cell encapsulation

Introduction

Elastic cartilage is a specialized connective tissue surrounded by perichondrium and characterized by the presence of chondrocytes immersed in an extracellular matrix (ECM) rich in elastic fibers and proteoglycans (Mills 2012). The three-dimensional organization of ECM molecules confers to the elastic cartilage its characteristic elasticity, flexibility and resistance to tensile and compression forces (Wu and Herzog 2002; Gaut and Sugaya 2015). In the human body, elastic cartilage is relatively abundant and can be found in the external part of the ear, external ear canal, Eustachian tube and larynx (epiglottis, Santorini's cartilage and Wrisberg cartilage) (Mills 2012).

Organs with elastic cartilage can be affected by neoplasms, traumatic injuries and congenital abnormalities, with functional and esthetic consequences for the patients. Unfortunately, elastic cartilage has a limited capacity to regenerate, and plastic and reconstructive surgical treatment is still challenging (Kuo et al. 2015; Hsiao et al. 2010). In external ear reconstruction, the standard surgical procedure consists of the use of autologous rib hyaline cartilage covered by a temporoparietal flap and skin graft (Brent 1999). This strategy is entirely autologous, with low risks of infections and good integration. However, autologous material is not always available, or may be insufficient. In addition, this method is technique-dependent and these procedures may cause donor-site morbidity or other clinical complications. Therefore, an effective treatment for

the reconstruction of tissues and organs composed of elastic cartilage is still needed (Chang et al. 2003).

Tissue engineering offers the possibility to generate different kinds of tissues or organs by using cells, biomaterials and growth factors (Carriel et al. 2012, 2014a; Garzon et al. 2012a; Silva et al. 2013). In recent years, several biomaterials have been used in cartilage tissue engineering, and it is currently accepted that these biomaterials should be biodegradable, biocompatible, nontoxic and mechanically stable (Nayyer et al. 2012). In addition, these biomaterials should allow chondrocytes to proliferate, migrate, differentiate and finally become integrated in vivo (Nayyer et al. 2012). Synthetic polymers have been used successfully to culture different kinds of chondrocytes (Oliveira et al. 2007; Oliveira and Reis 2011; Silva et al. 2013; Gaut and Sugaya 2015; Li and Hu 2015; Tsai et al. 2015). However, they are not biomimetic, are usually hydrophobic, have a long-term degradation period, and may release toxic metabolites; these drawbacks can hinder new cartilage regeneration (Nayyer et al. 2012; Li and Hu 2015; Liao et al. 2015).

Unfortunately, ideal biomaterials do not exist, and it is necessary to find suitable biomaterials for the generation of elastic cartilage substitutes. In this connection, a natural, biodegradable biomaterial called fibrin-agarose hydrogel (FAH) has emerged as a possible scaffold for cartilage tissue engineering. FAH have been used successfully to generate different three-dimensional tissue models with promising results (Alaminos et al. 2006; Carriel et al. 2012, 2014c, 2015; Garzon et al. 2014b; San Martin et al. 2013). Additionally, the fiber density and biomechanical properties of FAH can be regulated by using nanostructuration technique (Scionti et al. 2014; Carriel et al. 2015). These nanostructured FAH (NFAH) supported cells proliferation, migration and the synthesis of different ECM in engineered tissues ex vivo (Carriel et al. 2015; Ionescu et al. 2011). Based on the positive results obtained with NFAH in tissue engineering, the aims of this study were to evaluate the possibility of encapsulating human elastic cartilage-derived chondrocytes (HECDC) in NFAH for elastic cartilage tissue engineering, and to evaluate the capability of NFAH to support chondrocyte viability, proliferation and extracellular matrix synthesis.

Materials and methods

Cell culture and Live/Dead® cell viability assay

HECDC used in this study were obtained from small elastic cartilage biopsies from healthy young donors who underwent minor ear surgery. Once in the laboratory, biopsies were divided into two pieces, one for cell isolation and another used as a native control for histological analyses. Chondrocytes were isolated according to previously described protocols (Garzon et al. 2012a). Briefly, tissue samples were mechanically fragmented and then digested overnight in 2 mg/mL *Clostridium histolyticum* type II collagenase (Gibco BRL Life Sciences Technologies) at 37 °C. Approximately 5×10^5 HECDC were initially harvested by centrifugation and cultured with an expansion medium (EM) composed of a 3:1 mixture of DMEM and Ham's F12 culture medium supplemented with 10 % fetal bovine serum, 1 % antibiotic and an antimycotic cocktail solution (100 U/mL penicillin G, 100 mg/mL streptomycin and 0.25 mg/mL amphotericin B), 24 µg/mL adenine, 0.4 µg/mL hydrocortisone, 5 µg/mL insulin, 1.3 ng/mL triiodothyronine and 8 ng/mL cholera toxin (all from Sigma-Aldrich). The culture medium was replaced every 3 days, and HECDC were expanded until passage 10. This research project and the procedures were approved by the Ethic Committee of the Andalusian Public Health System in Granada (SAS PI-0653-2013).

In order to obtain an overall view of time-dependent cell viability, and to select viable cells for encapsulation in NFAH, HECDC cells from passages 1 to 10 were analyzed with the *Live/Dead® cell viability assay* (Viability/Cytotoxicity kit; Molecular Probes, UK) according to the manufacturer's guidelines and previous recommendations (Garzon et al. 2012a, b; Martin-Piedra et al. 2013, 2014). Briefly, cell viability was analyzed in triplicate by using three chamber slides (four chambers each) for each passage. Cells were seeded at 5×10^3 in each chamber and kept in culture for 48 h. After that, cells were rinsed with phosphate-buffered solution (PBS) and incubated with 200 µL Live/Dead solution for 30 min. Then cells were rinsed in PBS and examined in a Nikon Eclipse 90i fluorescence microscope. A total of ten images were obtained from each cell passage ($n = 30$ in each). Images were analyzed with the "analyze particles" function (particle size = 0−500 pixels^2) with ImageJ software (National Institute of Health, USA) as previously described (Carriel et al. 2015; Martin-Piedra et al. 2014).

In this study, HECDC from passage 2 were chosen for encapsulation in FAH based on well-known recommendations (Barbero et al. 2004; Hayes et al. 2007; Kessler and Grande 2008; Pappa et al. 2014) regarding the use of viable cells from early passages in order to avoid ex vivo chondrocyte dedifferentiation.

Encapsulation of HECDC in NFAH

FAH were prepared according to previously standardized protocols (Alaminos et al. 2006; Carriel et al. 2012, 2013, 2015). Briefly, to prepare a final volume of 60 mL FAH, we mixed 45.6 mL human plasma and 4.5 mL EM containing HECDC from passage 2. Then 900 µL

Amchafibrin (tranexamic acid; Fides-Ecofarma, Valencia, Spain) was added to prevent fibrinolysis. This solution was mixed and then 6 mL 2 % $CaCl_2$ and 3 mL type VII agarose (Sigma-Aldrich) were added and carefully mixed, and the resulting mixture was distributed in 6-well cell culture clusters (5 mL per well) and kept at 37 °C until complete gelation. As a result, we obtained cellular constructs 3 cm in diameter and 0.5 cm thick with 0.1 % of agarose, which were kept in culture for 24 h. In this study, two experimental groups were used based on cell density, and both were evaluated in triplicate. In experimental group A, 4.5×10^3 HECDC/mL were encapsulated, whereas in experimental group B, 45×10^3 HECDC/mL were used.

To fabricate NFAH, the cellular constructs were nanostructured according to recently described procedures (Carriel et al. 2015; Ionescu et al. 2011; Scionti et al. 2014). Briefly, cellular constructs were carefully removed from the culture flask, placed between two nylon filter membranes (0.22 μm; Merck–Millipore) and compressed between two pieces of Whatman filter paper. We applied mechanical pressure at 500 g for 2.5 min to obtain cellular NFAH constructs. In order to elucidate the chondrogenic potential of our NFAH and promote HECDC proliferation, the constructs were kept in culture conditions with only EM, but without any chondrogenic factors. The EM was replaced every 3 days. Samples were harvested in triplicate for histological analyses after 1, 2, 3, 4 and 5 weeks of ex vivo culture.

Histological evaluation

Native elastic cartilage (control group) and NFAH constructs were rinsed in PBS, fixed in 10 % buffered formalin, dehydrated, cleared, embedded in paraffin and sectioned at 5 μm thickness. Histological analysis was done with hematoxylin and eosin (H&E) staining. In addition, specific cellular and extracellular components were detected with histochemical or immunohistochemical methods.

The chondrogenic and mesenchymal lineage of HECDC was verified by the immunohistochemical identification of S-100 protein and vimentin, respectively (Carriel et al. 2014b; Yammani 2012). HECDC proliferation was verified by the immunohistochemical identification of proliferating cell nuclear antigen (PCNA) as previously described (Carriel et al. 2015; Rodriguez et al. 2013). Active actin cytoskeletal remodeling (associated with lamellipodia formation and cell migration) was evaluated by the identification of cortactin (cortical actin binding protein; Carriel et al. 2015; Ren et al. 2009). Finally, mitochondria were identified by using a monoclonal antibody against the surface of intact human mitochondria (Martinez-Outschoorn et al. 2012).

Synthesis of elastic fibers by the HECDC was histochemically analyzed with orcein staining (Alfonso-Rodriguez et al. 2014), and the synthesis of collagen type I and II was identified by immunohistochemistry. Proteoglycan deposition was assessed with an alcian blue histochemical method (Carriel et al. 2012; Oliveira et al. 2013; Carriel et al. 2015), and aggrecan, biglycan and versican were identified by immunohistochemistry. For each immunohistochemical reaction, negative controls were used by omitting the primary antibody. Native human elastic cartilage was used as a positive control group. 3,3′-Diaminobenzidine (DAB) was used for each immunohistochemical assay except for mitochondria, in which case DAB was used with nickel (gray-blue reaction). These procedures were performed at the same time under the same conditions to ensure reproducibility of the results. All technical information related to the antibodies used here is summarized in Table 1.

Quantitative and statistical analyses

The cell proliferation index was determined as the percentage of proliferative cells in each group, as described previously (Carriel et al. 2015). Briefly, three images were taken from three different slides at 400× magnification (area of 6×10^4 μm^2) and the number of PCNA-positive cells was calculated and expressed as a percentage.

For statistical analyses, we first analyzed the normality of cell viability and cell proliferation index values with the Shapiro–Wilk statistical test. Because the values were non-normally distributed, we used the Mann–Whitney nonparametric test to compare the values for cell viability (between the passages 1–10) and cell proliferation index (in each group and between the two experimental groups).

The results for each variable were expressed as the mean and standard deviation (SD), and all data were analyzed with SPSS 16.00 software. A value of $p < 0.05$ was considered statistically significant in two-tailed tests.

For the semiquantitative analysis of ECM molecules as determined by histochemistry and immunohistochemistry, three independent histologists evaluated each sample and scored the positive reactions as strong (+++), mild (++), slight (+), very slight (±) or negative (–), as previously described (Garzon et al. 2009, 2014a).

Results

Cell culture and cell viability in two dimensions

HECDC were successfully isolated with collagenase and expanded ex vivo with EM. These cells showed a polygonal morphology over time (from passage 1–10), which was

Table 1 Antibodies used for the immunohistochemical analysis

Antibodies	Dilution/ incubation	Pretreatment	Reference
Rabbit anti-S100 polyclonal	1:400 60 min	Citrate buffer pH 6 25 min at 95 °C	Dako Cytomation, Glostrup, Denmark. Product number: Z0311
Mouse anti-vimentin monoclonal clone V9	1:200 60 min	Citrate buffer pH 6 25 min at 95 °C	Sigma-Aldrich. St.Louis, MO.USA Product number: V6630
Mouse anti-PCNA monoclonal clone PC10	1:1000 60 min	Citrate buffer pH 6 25 min at 95 °C	Sigma-Aldrich St.Louis, MO.USA. Product number: P8825
Rabbit anti-cortactin monoclonal EP1922Y	1:100 60 min	EDTA buffer pH 8 25 min at 95 °C	ABCAM Cambridge UK. Product number: ab81208
Mouse anti mitochondria monoclonal clone 113-1	1:80 60 min	EDTA buffer pH 8 25 min at 95 °C	EMD Millipore, Darmstadt Germany Product number: MAB1273
Rabbit anti-collagen I. polyclonal	1:500 90 min	Pepsin 10 min 37 °C	Acris antibodies. Germany Product number: R1038
Rabbit anti-collagen II. polyclonal	1:250 Overnight 4 °C	Buffer EDTA pH 8 25 min at 95 °C	EMD Millipore. Billerica, Massachusetts.USA. Product number: AB2036
Mouse anti human aggrecan monoclonal.	1:250 60 min	Chondroitinase ABC 60 min 37 °C	AbD Serotec (Bio-Rad) Product number: MCA4722
Rabbit anti-biglycan polyclonal	1:100 60 min	Citrate buffer pH 6 25 min at 95 °C	ABCAM Cambridge UK. Product number: ab49701
Rabbit anti-versican polyclonal	1:100 Overnight 4 °C	Chondroitinase ABC 60 min 37 °C	ABCAM Cambridge UK. Product number: ab19345

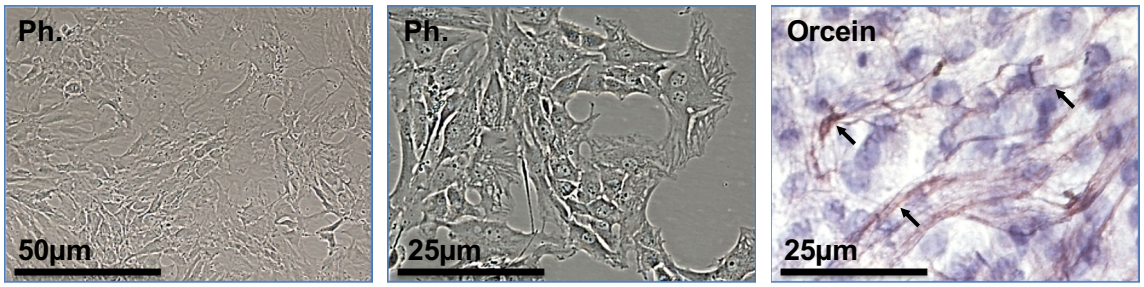

Live/Dead ® assay

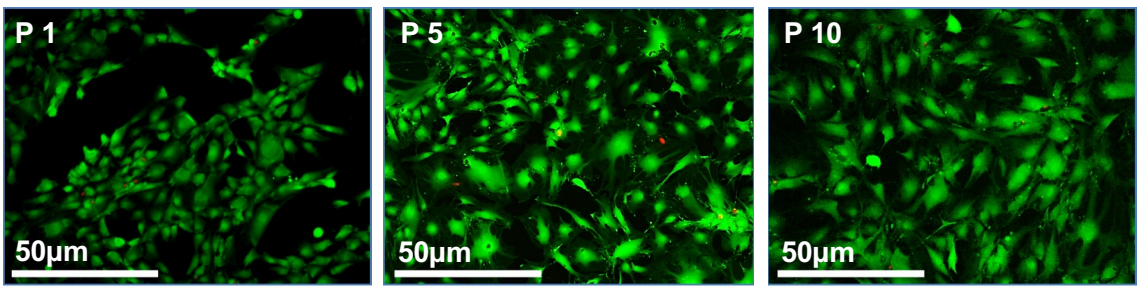

Passage	1	2	3	4	5	6	7	8	9	10
Mean	97.22	98.50	98.18	98.38	96.06	96.68	96.87	99.53	95.77	98.45
SD	1.96	0.48	0.97	1.09	2.62	1.72	2.30	0.41	1.97	0.70

Fig. 1 Morphological features and cell viability of HECDC. Phase contrast microscopy (Ph) and orcein histochemical staining of elastic fibers (*brown reaction*). Representative images of Live/Dead® cell viability assay (passages 1, 5 and 10) and mean ± standard deviation (SD) cell viability in each passage

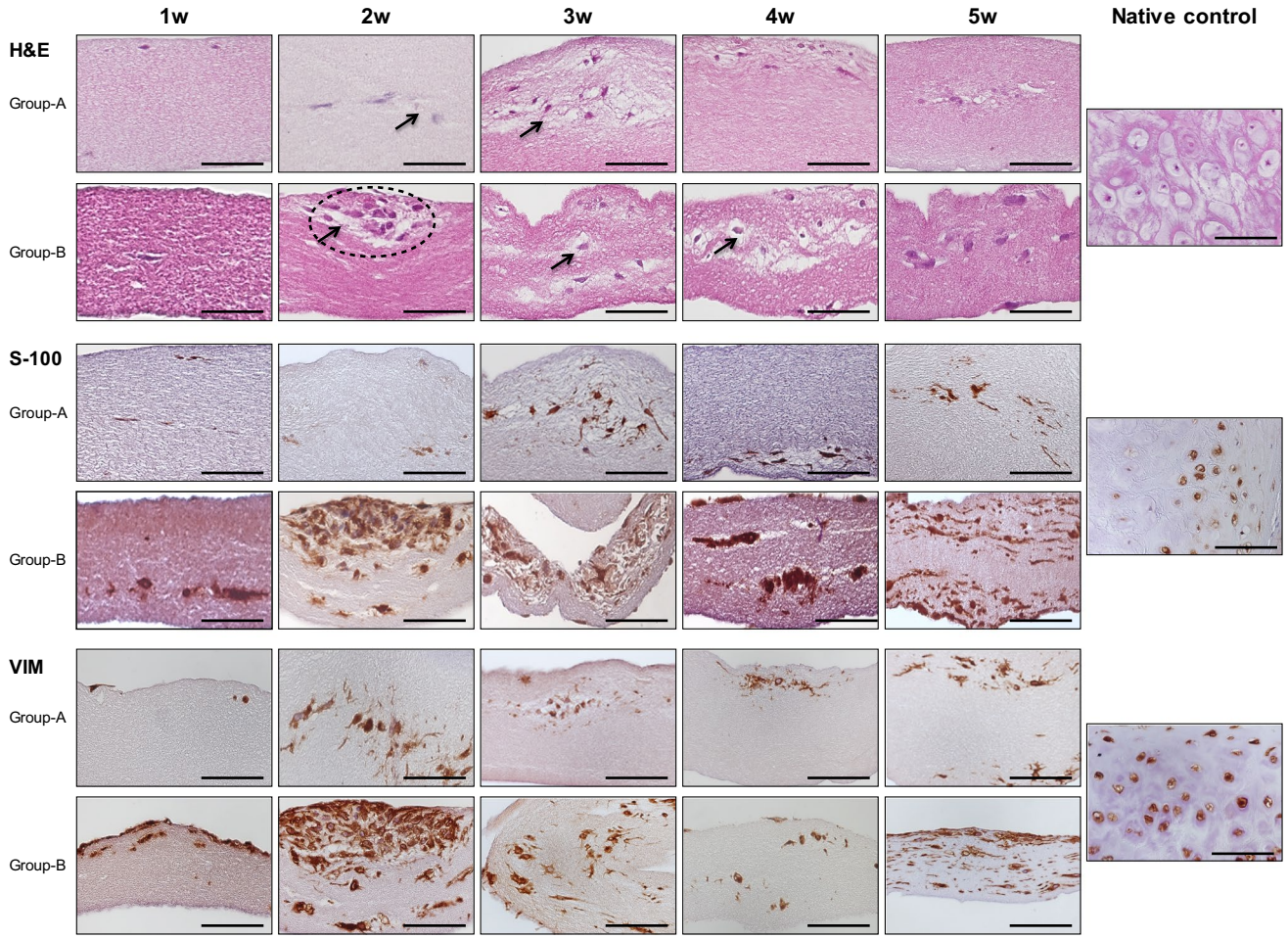

Fig. 2 Hematoxylin-eosin staining, S-100 and vimentin (VIM) expression by HECDC in NFAH. *Black arrows* indicate signs of scaffold degradation, and the *circle* shows a cell cluster. *Scale bar* 100 µm

characterized by the presence of one or two large central nuclei, wide lamellipodia and some short filopodia (Fig. 1). In addition, these cells synthesized elastic fibers in two-dimensional culture from passage 4 onward, which were histochemically identified by orcein staining (Fig. 1). The *Live/Dead® cell viability assay* showed high cell viability through all passages. Percentage cell viability ranged from 95 % to 99 % with a mean of 97.57 ± 1.22 %, with maximum values in passages 8 (99.53 %) and 2 (98.50 %). The cell viability observed in passage 8 was significantly higher than in other passages ($p < 0.05$), followed by passage 2, which was significantly higher than passages 5, 6 and 9 ($p < 0.05$) (see representative pictures and quantitative values in Fig. 1). In this study, HECDC from passage 2 were chosen for encapsulation in NFAH, since this was the earliest passage with high cell viability and therefore, the risk of dedifferentiation (often observed in late cell passages) was lower.

Histology, histochemistry and immunohistochemistry

H&E staining revealed that HECDC were successfully encapsulated in NFAH, and both cells and biomaterial fibers showed a random distribution. In addition, we observed a steady increase in the number of HECDC with time in both experimental groups, especially in group B. In group A, this increase was especially evident during the first 3 weeks, but less clear between weeks 4 and 5 of development ex vivo. HECDC showed an irregular morphology (elongated to spheroid) and formed cell clusters (Fig. 2). Interestingly, from the second week onward, signs of biomaterial degradation were observed in both groups, which were more evident between and around the cluster-forming chondrocytes in group B (Fig. 2). When the chondrogenic and mesenchymal lineage of the HECDC was evaluated, immunohistochemical analyses revealed an intense positive reaction for S-100 protein and vimentin. The cytoplasmic

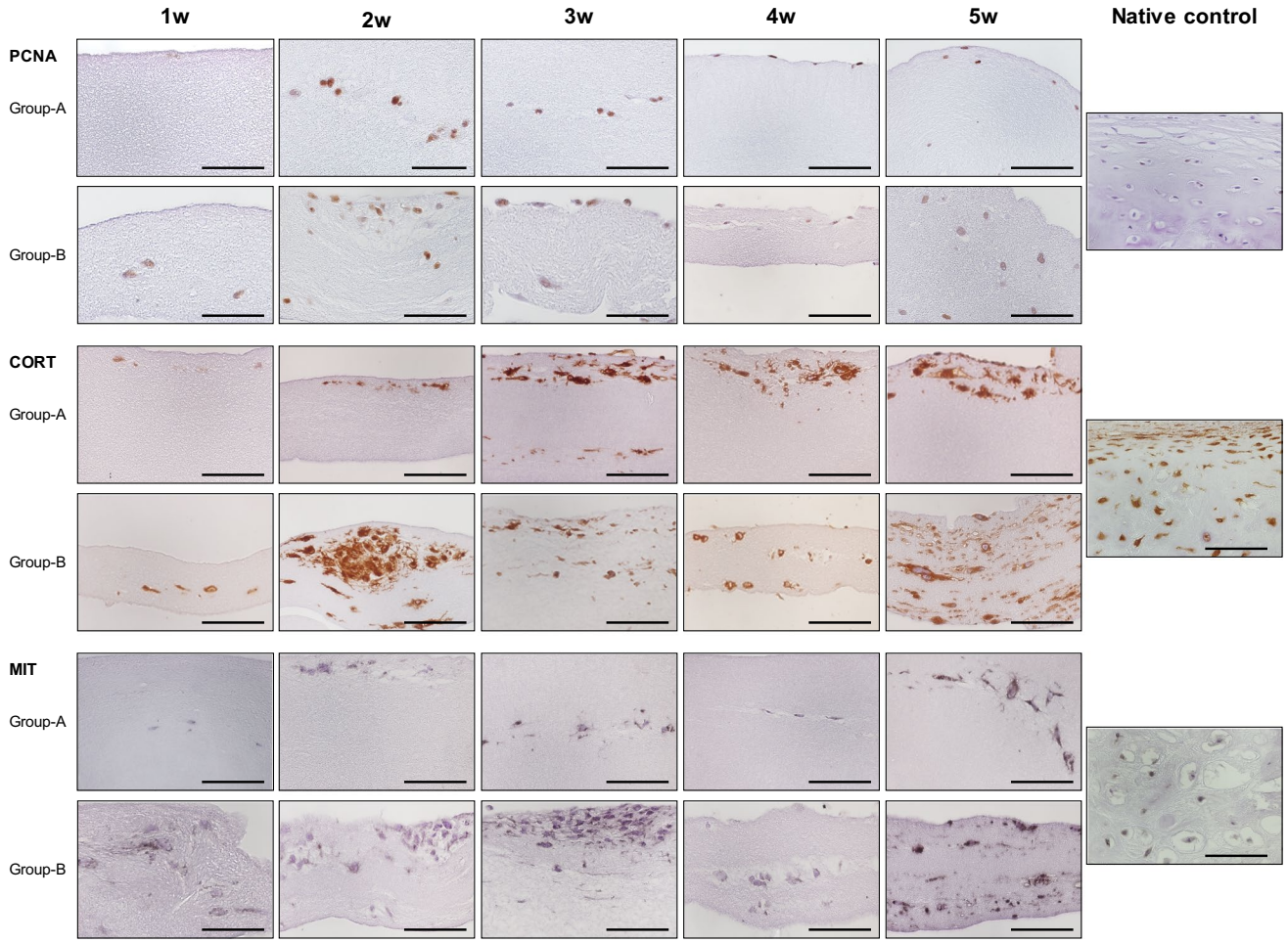

Fig. 3 Immunohistochemical analyses of PCNA, cortactin and mitochondria expression by encapsulated HECDC. In mitochondria, DAB with nickel was used (*gray-blue positive reaction*). *Scale bar* 100 µm

pattern of both proteins confirmed the irregular morphology of the encapsulated HECDC (Fig. 2).

Analysis of cell proliferation with PCNA showed that HECDC were able to proliferate in both groups with time (Fig. 3). In addition, the cell proliferation index revealed slight differences in time and between the two experimental groups (Figs. 3, 4). In group A, quantitative analysis revealed that the cell proliferation index decreased significantly ($p < 0.05$) from the first week (100 % positive cells) to the fifth week (86 % positive cells) of ex vivo development. Strikingly, the lowest cell proliferation index was observed in week 3 (59 % positive cells), but quantitative analysis showed a steady and significant recovery of these values ($p < 0.05$) between the fourth and fifth weeks (Fig. 4). Similarly, in group B, a significant decrease in cell proliferation index was observed between the first and fifth week ($p < 0.05$), when this value reached 44 %. As found in group A, a slight increase in cell proliferation index occurred between the fourth and fifth weeks, but this increase was not statistically significant ($p > 0.05$; Fig. 4). When we compared cell proliferation index between the two experimental groups, higher values were observed in group A for all weeks. However, these differences were only significant for the first, fourth and fifth weeks of ex vivo development (Fig. 4). In native control, PCNA staining was weak (Fig. 3).

Cortactin immunohistochemical analysis showed a steady increase in the positive reaction in the cytoplasm of HECDC from the second week onward in both groups. Interestingly, the cytoplasmic pattern found ex vivo was comparable to the positive reaction in native control cartilage (Fig. 3).

Mitochondria analysis revealed that HECDC were able to generate and maintain these vital organelles from the second week in group A and from the first week in group B. In group B, a steady increase in the immunoreactions was observed, especially in cluster-forming chondrocytes. Surprisingly, the immunoreactivity for mitochondria was more abundant and intense in group B than in group A and the native control, in which this immunoreaction was weaker (Fig. 3).

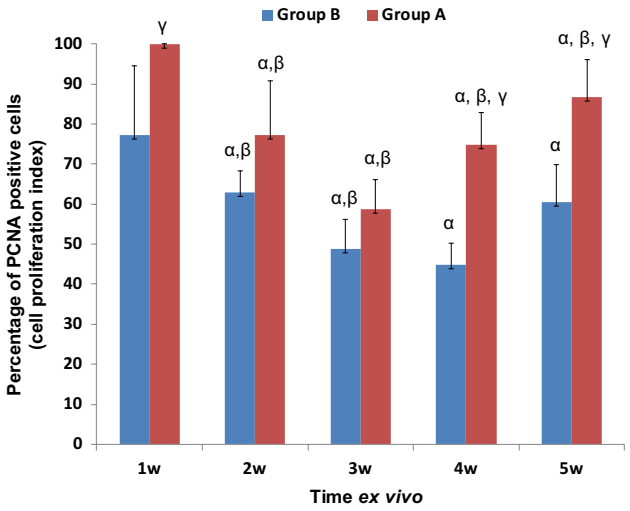

Fig. 4 Graphic representation of cell proliferation index in both experimental groups during ex vivo development. Note the decrease in mean values, which was followed by a steady increase in both experimental groups. α = Differences versus first week in each group were statistically significant. β = Differences versus the previous week in each group were statistically significant. γ = Differences between Group A and Group B in each week were statistically significant

The capacity of HECDC in NFAH to synthesize ECM was analyzed qualitatively and semiquantitatively (Table 2) by histochemistry and immunohistochemistry. Orcein staining showed an intense reaction for elastic fibers in the native control. In group A, we observed very slight expression at 3 weeks. In contrast, cells in group B were able to synthesize elastic fibers from the first week, with an intense extracellular positive reaction around cluster-forming chondrocytes (Fig. 5). For collagen type I, the immunohistochemical analysis revealed positive expression in the native control and in both experimental groups. In group A, collagen type I was observed from the second week, and expression increased steadily with time, especially around cluster-forming chondrocytes (Fig. 5). In group B, collagen type I expression started in the first week and was more abundant than in group A (Fig. 5). Regarding the expression pattern of collagen type I, both groups showed extracellular staining (Fig. 5, Table 2), but some cells also showed a positive reaction in the cytoplasm (data not shown). Collagen type II expression was positive in the native control and in both experimental groups, but the distribution and intensity of this protein were lower than for collagen type I in both experimental groups. Collagen type II expression started in week 2 ex vivo and was more abundant in group B than group A (Fig. 5; Table 2). In addition, expression was more intense and abundant around and between the cluster-forming chondrocytes.

The histochemical evaluation of acid proteoglycans with alcian blue staining showed an intense and widely distributed positive reaction at the extracellular level in native control.

Table 2 Semiquantitative analysis of ECM molecules by histochemistry and immunohistochemistry

Staining/groups	1 w	2w	3w	4w	5w	Native CTR
Orcein						
A	–	–	±	±	–	+++
B	++	+++	++	+	+	
Collagen type I						
A	–	+	+++	+++	+++	+++
B	±	+++	++	+	+++	
Collagen type II						
A	–	–	–	±	+	++
B	–	++	+	+	+	
Alcian blue						
A	–	–	+	–	–	+++
B	±	±	–	±	–	
Aggrecan						
A	–	–	++	–	–	++
B	–	++	–	–	–	
Biglycan						
A	–	+	+	++	++	+++
B	–	++	++	±	+	
Versican						
A	–	+	+	+	++	+
B	±	++	+	±	±	

Positive reactions were scored as strong (+++), mild (++), slight (+), very slight (±) or negative (–)

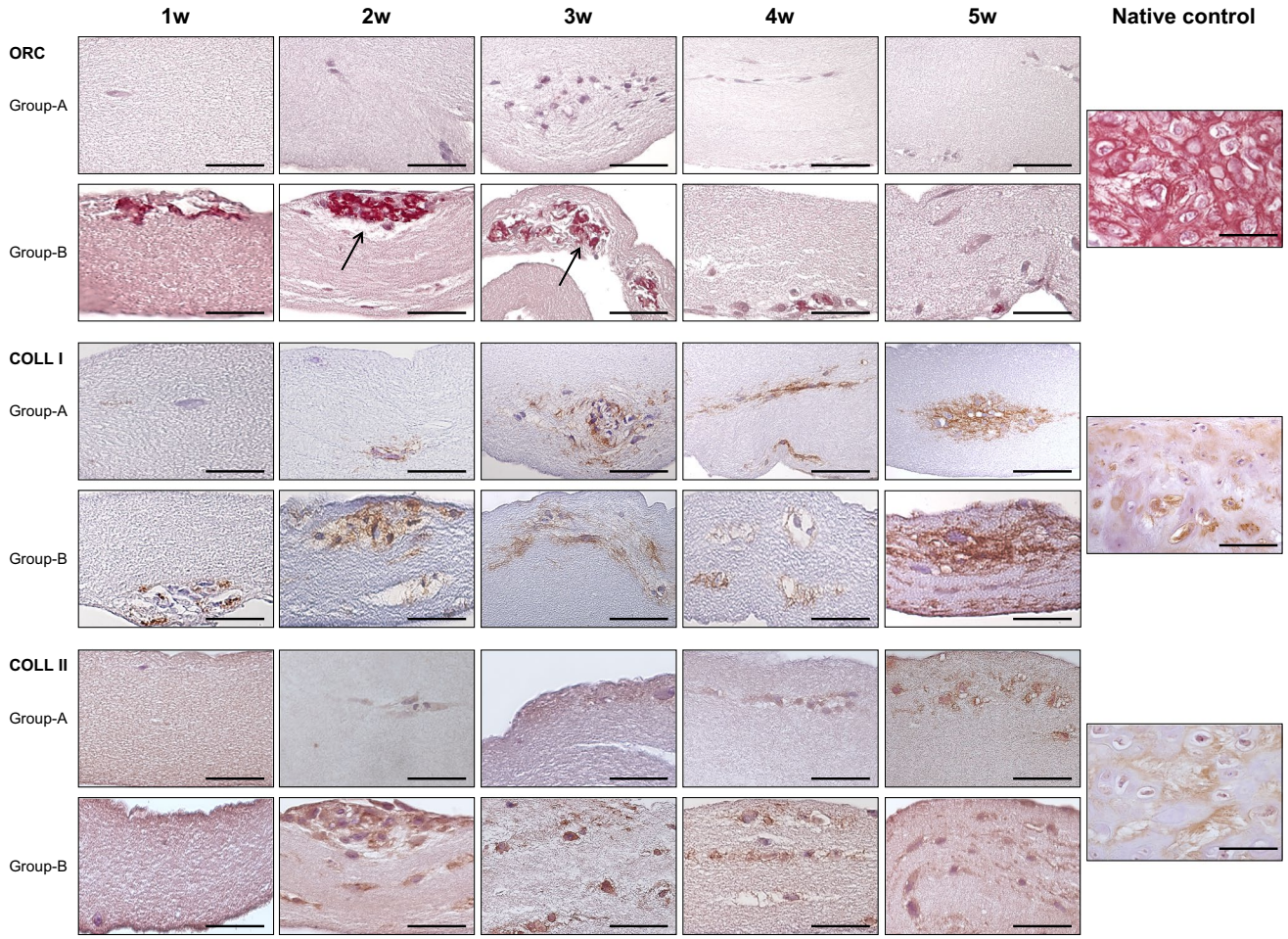

Fig. 5 Histochemical and immunohistochemical analyses of ECM fibers synthesized by encapsulated HECDC. *Arrows* show the positive histochemical reaction for elastic fibers with orcein (ORC). *COLL I* and *COLL II* show collagen type I and II, respectively. *Scale bar* 100 µm

In the experimental groups, staining was slightly positive, especially in the cell clusters. However, we observed no differences in the intensity of alcian blue staining between the two experimental groups (Fig. 6; Table 2). The immunohistochemical analysis for aggrecan showed a positive reaction in the native control and in both experimental groups. In the experimental groups, the positive reaction for aggrecan was restricted to the intercellular matrix between cluster-forming chondrocytes (Fig. 6; Table 2). Proteoglycan biglycan expression was also positive in the native control and in both experimental groups. Biglycan was first expressed from week 2 onward with a clear pericellular pattern in both experimental groups (Fig. 6; Table 2). We also evaluated the synthesis of the proteoglycan versican. In the native control, versican was seen mainly in the perichondrium and was less strongly expressed in mature chondrocytes. Versican was synthesized steadily from the first to the fifth week in group A. In group B, high levels of versican were observed in the first two weeks, but this proteoglycan tended to decrease with time (Fig. 6; Table 2).

Discussion

Here we isolated, selected and encapsulated HECDC in NFAH for its possible use in cartilage tissue engineering, and evaluated cell-biomaterial interactions during 5 weeks with histological techniques.

HECDC were successfully isolated with collagenase type II as previously described (Garzon et al. 2012a). The encapsulated chondrocytes showed a high percentage of cell viability (*Live/Dead® cell viability assay*) during two-dimensional expansion (mean 97 % over 10 passages), with maximum values in passages 2 and 8. Our results are consistent with those of other authors in elastic cartilage-derived rabbit chondrocytes (Garcia-Lopez et al. 2015) and human fibrochondrocytes (Garzon et al. 2012a). Chondrocytes are known to tend to dedifferentiate during ex vivo expansion (Barbero et al. 2004; Garzon et al. 2012a; Johnstone et al. 2013; Kessler and Grande 2008), and for this reason, earlier authors recommended the use of viable chondrocytes from earlier cell passages (Barbero

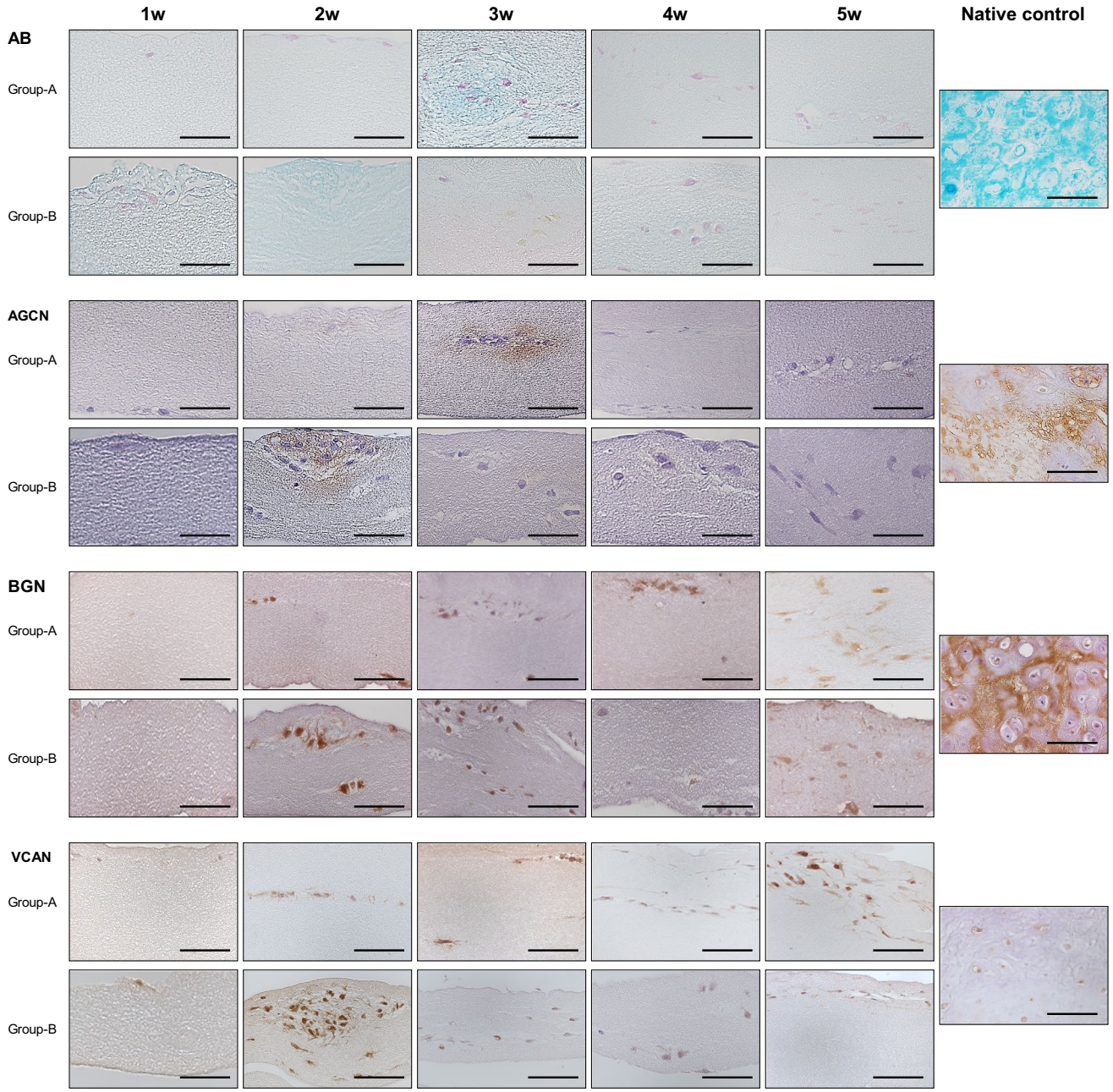

Fig. 6 Histochemical and immunohistochemical analyses of proteoglycans synthesized by encapsulated HECDC. AB = alcian blue histochemical staining for acid proteoglycans. *AGCN*, *BGN* and *VCAN* show the immunohistochemical identification of aggrecan, biglycan and versican, respectively. *Scale bar* 100 µm

et al. 2004; Bhattacharjee et al. 2015; Hayes et al. 2007; Kessler and Grande 2008; Garzon et al. 2012a). Based on this information, we used highly viable HECDC from the second passage in this study for encapsulation in NFAH. The number of cells available at this passage was limited, but could be increased by using larger-sized elastic cartilage biopsies. Unfortunately, we did not evaluate the phenotype of HECDC in this study. Therefore, more studies are needed to characterize the dedifferentiation phenotype of elastic cartilage-derived chondrocytes for use in tissue engineering.

In recent years, different biomaterials have been studied for the culture, seeding or encapsulation of chondrocytes derived from elastic cartilage. In this context, synthetic biomaterials such as polyglycolic acid (PGA), polycaprolactone (PCL) or poly-L-lactic acid (PLLA), which offer well-known biomechanical properties, have been studied most frequently (Kusuhara et al. 2009; Liu et al. 2010; Zhao

et al. 2015). However, their in vivo degradation can create an adverse microenvironment which may cause chronic inflammation, tissue degradation and/or even tissue necrosis (Carriel et al. 2014a; Kusuhara et al. 2009; Liu et al. 2010; Zhao et al. 2015). In this regard, the natural biomaterial FAH offers high biocompatibility and biodegradability and supports different cell functions such as proliferation, differentiation, migration and ECM synthesis ex vivo and in vivo (Alaminos et al. 2006; Carriel et al. 2012, 2013, 2014c, 2015; Garzon et al. 2014b; San Martin et al. 2013). From the biomechanical point of view, FAH are considered a versatile biomaterial, and its biomechanical properties can be adjusted and tuned over a broad range by changing the hydration rate of the biomaterial with nanostructuration techniques, modifying the agarose content, forming multilayered three-dimensional structures, and the incorporation of magnetic nanoparticles. Therefore, the biomechanical properties of these constructs may vary between 5 and 460 kPa for Young's modulus, 1–75 kPa for the elastic compression modulus, 4–3100 Pa for G value, 15–4750 Pa for G' and 2–600 Pa for G'' (Carriel et al. 2015; Ionescu et al. 2011; Lopez–Lopez et al. 2015; Rodriguez et al. 2013; Rodriguez-Arco et al. 2016).

Our histological analyses demonstrate that encapsulated HECDC in NFAH were able to proliferate, but lost their typical chondrocyte morphology and acquired an irregular and/or elongated shape. These findings are supported by other studies done under two-dimensional and three-dimensional culture conditions (Garcia-Lopez et al. 2015; Garzon et al. 2012a; Yanaga et al. 2012; Zhao et al. 2015). Morphological changes are a sign of dedifferentiation, and can be explained by the absence of mechanical stimuli, the lack of a highly specialized ECM and the lack of a chondrogenic differentiation medium, which is often used to maintain chondrogenic differentiation and cell function (Garzon et al. 2012a; Yanaga et al. 2012). Despite its potential drawbacks, the use of an expansion medium in this study allowed us to determine the capability of NFAH to support cell growth, proliferation and ECM component synthesis. Future studies should be carried out with chondrogenic differentiation medium to analyze the differentiation status of cells immersed in NFAH and their capacity to generate cartilage tissue-like substitutes. In addition, most cells in the NFAH biomaterial were unevenly distributed, but cells tended to form clusters with time. Uneven distribution is a common finding in bioengineered tissues based on hydrogels such as collagen and fibrin-agarose scaffolds (Alaminos et al. 2006; Carriel et al. 2012, 2015; Cheema and Brown 2013; Garzon et al. 2014b).

In our study, although HECDC lost their typical morphology, they expressed S-100 and vimentin, especially at higher cell densities (group B). S-100 is expressed by Schwann cells (Carriel et al. 2013, 2014b), melanocytes and chondrocytes (Yammani 2012). In cartilage, S-100 can be found in different stages of chondrocyte maturation (Yammani 2012), especially in chondrocytes near damaged areas (Leonardi et al. 2000; Yammani 2012). Vimentin is a cytoskeletal intermediate filament of mesenchymal-derived cells and plays a structural role in chondrocytes (Mills 2012). The presence of S-100 and vimentin in both native control and HECDC encapsulated in NFAH suggests that HECDC retained some level of chondrogenic and mesenchymal lineage differentiation in NFAH.

Regarding cell proliferation, quantitative PCNA analysis revealed that HECDC were able to proliferate with time, although proliferation slowed in the third week in group B and in the fourth week in group A. Thereafter, both groups showed increased cell proliferation, which was significant in group A. Strikingly, HECDC encapsulated at low densities (group A) had a significantly higher cell proliferation index than cells at a higher density (group B). This can probably be explained by the cluster organization of these cells, which may repress cell proliferation due to contact inhibition. Other studies with FAH also reported an initial decrease in cell proliferation followed by a steady increase (Carriel et al. 2015; Rodriguez et al. 2013). Our results show that NFAH supported HECDC proliferation when expansion medium was used. This strategy is potentially useful to avoid the need to expand cells under two-dimensional culture conditions for prolonged periods. Although we used PCNA to evaluate cell proliferation, it is important to note that this protein has a longer life span than other proliferative markers such as Ki-67, and therefore our results may have been slightly overestimated.

With regard to cell attachment and migration, cells need to remodel their cytoskeleton in order to generate cytoplasmic protrusions, establish focal contact (attachment) and finally migrate through tissues or biomaterials. In this connection, cortactin acts as a regulatory protein that may coordinate the molecular components of the protrusive apparatus into a cohesive module (Ren et al. 2009). It was recently shown that cortactin is expressed by metabolically active and migrating mesenchymal stem cells cultured in FAH, but this expression decreased transitorily when these cells were immersed in multilayered NFAH (Carriel et al. 2015). In this study, HECDC consistently showed increasing expression of cortactin in both experimental groups, suggesting that these cells were able to remodel their cytoskeleton and were thus probably able to migrate into NFAH. In addition, encapsulated HECDC showed a steady increase in the positive reaction for human mitochondria, suggesting that these cells were metabolically active in NFAH ex vivo.

Elastic cartilage has a highly specialized ECM mainly composed of elastic fibers, collagen type II and large amounts of proteoglycans and aggrecan (Gentili and Cancedda 2009;

Kiani et al. 2002; Kreis and Vale 1999; Roughley 2006). In general, engineered elastic cartilage substitutes are kept under culture conditions for short periods and then tested subcutaneously in animal models (Chang et al. 2003; Garcia-Lopez et al. 2015; Liao et al. 2015; Zhao et al. 2015). Unfortunately, earlier studies did not demonstrate whether the elastic cartilage-derived chondrocytes synthetized essential ECM molecules ex vivo, although a steady increase in some ECM molecules was seen after some weeks in vivo (Chang et al. 2003; Garcia-Lopez et al. 2015; Liao et al. 2015; Zhao et al. 2015). In this connection, our results show that encapsulated HECDC have the capability to synthesize elastic and collagen type I and II fibers in NFAH. Elastic fibers and collagens were mainly produced by HECDC when they were encapsulated at higher cellular densities (group B), and especially when the cells formed clusters. Although these cells synthetized ECM molecules, our semiquantitative analysis showed that these positive reactions were not equivalent to the positive reactions observed in native control. Concerning the ECM composition of elastic cartilage, elastic fibers and collagen type II are characteristic components of this tissue (Gentili and Cancedda 2009; Kreis and Vale 1999; Mills 2012). Interestingly, some recent studies reported collagen type I expression in native elastic cartilage and in cultured elastic cartilage-derived chondrocytes (Pappa et al. 2014; Yanaga et al. 2012; Gentili and Cancedda 2009). However, collagen type I should not be considered a specific marker for elastic cartilage. The synthesis of the three main fibrillar ECM molecules of elastic cartilage by the HECDC in NFAH confirms that NFAH partially supported synthesis functions in these cells. Our results are consistent with previous studies in which FAH and NFAH supported the ex vivo synthesis of a range of ECM molecules by different types of cell (Carriel et al. 2012, 2015; Garzon et al. 2014b; Ionescu et al. 2011; San Martin et al. 2013).

Proteoglycans and aggrecan are essential molecules for normal function and nutrition in cartilage tissue (Kiani et al. 2002; Kreis and Vale 1999), although most proteoglycans can be found in different tissues and so are not specific to elastic cartilage. Alcian blue histochemical analysis revealed a weak reaction for these components in both experimental groups, in contrast to the intense reaction in native control. The immunohistochemical analysis of aggrecan revealed that cluster-forming chondrocytes were able to synthesize this molecule in an extracellular pattern, albeit at a lower level than native controls. In contrast, the expression of versican and especially biglycan was more widely distributed than aggrecan, and both showed a mainly pericellular distribution in a pattern that was comparable to collagen type II. Biglycan is a small leucine-rich proteoglycan (SLRP) found in several tissues including cartilage (Kreis and Vale 1999). Biglycan is not related to aggrecan in the cartilage (Roughley 2006), but it closely interacts with fibrillar collagens (types I, II and III), and thus supports fibril–fibril interaction and extracellular collagen arrangement (Giachini et al. 2008; Kreis and Vale 1999; Roughley 2006). Versican, which is present in several tissues such as central nervous system, skin, blood vessels and cartilage, can interact with collagens and/or aggrecan (Matsumoto et al. 2006). Indeed, versican serves as a temporary framework for aggrecan and collagen organization in developing cartilage (Matsumoto et al. 2006). In this connection, versican promotes cell proliferation, attachment and migration in several tissues during development (Kreis and Vale 1999; Matsumoto et al. 2006; Wight 2002). Our finding of biglycan expression by HECDC in NFAH and its expression pattern, which was comparable to that of collagens, suggests that this proteoglycan can support ex vivo collagen fibril–fibril interaction and reorganization in the NFAH. At the same time, versican may provide transitory support for aggrecan organization or collagen organization, but our results suggest that it is more closely associated with HECDC proliferation, attachment or even migration in NFAH ex vivo.

In conclusion, this study reports the successful testing of a method to encapsulate HECDC into thin biodegradable and natural fibrin-agarose hydrogels by using nanostructuration techniques. From a biological standpoint, our histological study suggests that nanostructured fibrin-agarose hydrogels are suitable biomaterials for cell encapsulation. Although HECDC partially lost their chondrogenic phenotype, these cells were able to proliferate, form cell clusters and synthesize different ECM molecules ex vivo without any chondrogenic medium. These preliminary results suggest that tissue-like nanostructured fibrin-agarose hydrogels are potentially useful in elastic cartilage tissue engineering. However, further biomechanical characterization, cell differentiation studies and preclinical in vivo studies are still needed to further test the potential use of these tissue-like constructs in elastic cartilage repair.

Acknowledgments This study was supported by the *Fundación Pública Andaluza Progreso y Salud, Consejería de Salud, Junta de Andalucía*, *España*, Grant PI-0653-2013. The authors thank K. Shashok for assistance with the English in the manuscript. In addition, Prof. Víctor Carriel is grateful to "*Comisión Nacional de Investigación Científica y Tecnológica (CONICYT), programa de Becas Chile, del Gobierno de Chile*". This work forms part of the doctoral thesis by Laura García-Martínez.

Compliance with ethical standard

Conflict of interest The authors declare no conflicts of interest.

References

Alaminos M, Del Carmen Sanchez-Quevedo M, Munoz-Avila JI, Serrano D, Medialdea S, Carreras I, Campos A (2006) Construction

of a complete rabbit cornea substitute using a fibrin-agarose scaffold. Invest Ophthalmol Vis Sci 47(8):3311–3317. doi:10.1167/iovs.05-1647

Alfonso-Rodriguez CA, Garzon I, Garrido-Gomez J, Oliveira AC, Martin-Piedra MA, Scionti G, Carriel V, Hernandez-Cortes P, Campos A, Alaminos M (2014) Identification of histological patterns in clinically affected and unaffected palm regions in dupuytren's disease. PLoS ONE 9(11):e112457. doi:10.1371/journal.pone.0112457

Barbero A, Grogan S, Schafer D, Heberer M, Mainil-Varlet P, Martin I (2004) Age related changes in human articular chondrocyte yield, proliferation and post-expansion chondrogenic capacity. Osteoarthritis Cartilage/OARS Osteoarthritis Res Soc 12(6):476–484. doi:10.1016/j.joca.2004.02.010

Bhattacharjee M, Coburn J, Centola M, Murab S, Barbero A, Kaplan DL, Martin I, Ghosh S (2015) Tissue engineering strategies to study cartilage development, degeneration and regeneration. Adv Drug Deliv Rev 84:107–122. doi:10.1016/j.addr.2014.08.010

Brent B (1999) Technical advances in ear reconstruction with autogenous rib cartilage grafts: personal experience with 1200 cases. Plast Reconstr Surg 104(2):319–334

Carriel V, Garzon I, Jimenez JM, Oliveira AC, Arias-Santiago S, Campos A, Sanchez-Quevedo MC, Alaminos M (2012) Epithelial and stromal developmental patterns in a novel substitute of the human skin generated with fibrin-agarose biomaterials. Cells Tissues Organs 196(1):1–12. doi:10.1159/000330682

Carriel V, Garrido-Gomez J, Hernandez-Cortes P, Garzon I, Garcia-Garcia S, Saez-Moreno JA, Del Carmen Sanchez-Quevedo M, Campos A, Alaminos M (2013) Combination of fibrin-agarose hydrogels and adipose-derived mesenchymal stem cells for peripheral nerve regeneration. J Neural Eng 10(2):026022. doi:10.1088/1741-2560/10/2/026022

Carriel V, Alaminos M, Garzon I, Campos A, Cornelissen M (2014a) Tissue engineering of the peripheral nervous system. Expert Rev Neurother 14(3):301–318. doi:10.1586/14737175.2014.887444

Carriel V, Garzon I, Alaminos M, Cornelissen M (2014b) Histological assessment in peripheral nerve tissue engineering. Neural Regen Res 9(18):1657–1660. doi:10.4103/1673-5374.141798

Carriel V, Garzon I, Campos A, Cornelissen M, Alaminos M (2014c) Differential expression of GAP-43 and neurofilament during peripheral nerve regeneration through bio-artificial conduits. J Tissue Eng Regen Med. doi:10.1002/term.1949

Carriel V, Scionti G, Campos F, Roda O, Castro B, Cornelissen M, Garzon I, Alaminos M (2015) In vitro characterization of a nanostructured fibrin agarose bio-artificial nerve substitute. J Tissue Eng Regen Med. doi:10.1002/term.2039

Chang SC, Tobias G, Roy AK, Vacanti CA, Bonassar LJ (2003) Tissue engineering of autologous cartilage for craniofacial reconstruction by injection molding. Plast Reconstr Surg 112(3):793–799. doi:10.1097/01.PRS.0000069711.31021.94

Cheema U, Brown RA (2013) Rapid fabrication of living tissue models by collagen plastic compression: understanding three-dimensional cell matrix repair. Adv Wound Care (New Rochelle) 2(4):176–184. doi:10.1089/wound.2012.0392

Garcia-Lopez J, Garciadiego-Cazares D, Melgarejo-Ramirez Y, Sanchez-Sanchez R, Solis-Arrieta L, Garcia-Carvajal Z, Sanchez-Betancourt JI, Ibarra C, Luna-Barcenas G, Velasquillo C (2015) Chondrocyte differentiation for auricular cartilage reconstruction using a chitosan based hydrogel. Histol Histopathol 30(12):1477–1485. doi:10.14670/HH-11-642

Garzon I, Serrato D, Roda O, Del Carmen Sanchez-Quevedo M, Gonzales-Jaranay M, Moreu G, Nieto-Aguilar R, Alaminos M, Campos A (2009) In vitro cytokeratin expression profiling of human oral mucosa substitutes developed by tissue engineering. Int J Artif Organs 32(10):711–719

Garzon I, Carriel V, Marin-Fernandez AB, Oliveira AC, Garrido-Gomez J, Campos A, del Carmen Sanchez-Quevedo M, Alaminos M (2012a) A combined approach for the assessment of cell viability and cell functionality of human fibrochondrocytes for use in tissue engineering. PLoS ONE 7(12):e51961. doi:10.1371/journal.pone.0051961

Garzon I, Perez-Kohler B, Garrido-Gomez J, Carriel V, Nieto-Aguilar R, Martin-Piedra MA, Garcia-Honduvilla N, Bujan J, Campos A, Alaminos M (2012b) Evaluation of the cell viability of human Wharton's jelly stem cells for use in cell therapy. Tissue Eng Part C Methods 18(6):408–419. doi:10.1089/ten.TEC.2011.0508

Garzon I, Alfonso-Rodriguez CA, Martinez-Gomez C, Carriel V, Martin-Piedra MA, Fernandez-Valades R, Sanchez-Quevedo MC, Alaminos M (2014a) Expression of epithelial markers by human umbilical cord stem cells. Topogr Anal Placent 35(12):994–1000. doi:10.1016/j.placenta.2014.09.007

Garzon I, Martin-Piedra MA, Alfonso-Rodriguez C, Gonzalez-Andrades M, Carriel V, Martinez-Gomez C, Campos A, Alaminos M (2014b) Generation of a biomimetic human artificial cornea model using Wharton's jelly mesenchymal stem cells. Invest Ophthalmol Vis Sci 55(7):4073–4083. doi:10.1167/iovs.14-14304

Gaut C, Sugaya K (2015) Critical review on the physical and mechanical factors involved in tissue engineering of cartilage. Regen Med 10(5):1–15. doi:10.2217/rme.15.31

Gentili C, Cancedda R (2009) Cartilage and bone extracellular matrix. Curr Pharm Des 15(12):1334–1348

Giachini FR, Carriel V, Capelo LP, Tostes RC, Carvalho MH, Fortes ZB, Zorn TM, San Martin S (2008) Maternal diabetes affects specific extracellular matrix components during placentation. J Anat 212(1):31–41. doi:10.1111/j.1469-7580.2007.00839.x

Hayes AJ, Hall A, Brown L, Tubo R, Caterson B (2007) Macromolecular organization and in vitro growth characteristics of scaffold-free neocartilage grafts. J Histochem Cytochem Off J Histochem Soc 55(8):853–866. doi:10.1369/jhc.7A7210.2007

Hsiao HT, Leu YS, Tung KY (2010) Epiglottis reconstruction with free radial forearm flap after supraglottic laryngectomy. Am J Otolaryngol 31(2):132–135. doi:10.1016/j.amjoto.2008.11.004

Ionescu AM, Alaminos M, de la Cruz Cardona J, de DiosGarcia-LopezDuran J, Gonzalez-Andrades M, Ghinea R, Campos A, Hita E, del Mar Perez M (2011) Investigating a novel nanostructured fibrin-agarose biomaterial for human cornea tissue engineering: rheological properties. J Mech Behav Biomed Mater 4(8):1963–1973. doi:10.1016/j.jmbbm.2011.06.013

Johnstone B, Alini M, Cucchiarini M, Dodge GR, Eglin D, Guilak F, Madry H, Mata A, Mauck RL, Semino CE, Stoddart MJ (2013) Tissue engineering for articular cartilage repair—the state of the art. Eur Cell Mater 25:248–267

Kessler MW, Grande DA (2008) Tissue engineering and cartilage. Organogenesis 4(1):28–32

Kiani C, Chen L, Wu YJ, Yee AJ, Yang BB (2002) Structure and function of aggrecan. Cell Res 12(1):19–32. doi:10.1038/sj.cr.7290106

Kreis T, Vale R (1999) Guidebook to the extracellular matrix, anchor, and adhesion proteins, 2nd edn. Oxford University Press, Oxford England, New York

Kuo CY, Huang BR, Chen HC, Shih CP, Chang WK, Tsai YL, Lin YY, Tsai WC, Wang CH (2015) Surgical results of retrograde mastoidectomy with primary reconstruction of the ear canal and mastoid cavity. Biomed Res Int 2015:517035. doi:10.1155/2015/517035

Kusuhara H, Isogai N, Enjo M, Otani H, Ikada Y, Jacquet R, Lowder E, Landis WJ (2009) Tissue engineering a model for the human ear: assessment of size, shape, morphology, and gene expression following seeding of different chondrocytes. Wound Repair Regen 17(1):136–146. doi:10.1111/j.1524-475X.2008.00451.x

Leonardi R, Villari L, Bernasconi G, Piacentini C, Baciliero U, Travali S (2000) Cellular S-100 protein immunostaining in human dysfunctional temporomandibular joint discs. Arch Oral Biol 45(5):411–418

Li KC, Hu YC (2015) Cartilage tissue engineering: recent advances and perspectives from gene regulation/therapy. Adv Healthc Mater 4(7):948–968. doi:10.1002/adhm.201400773

Liao HT, Zheng R, Liu W, Zhang WJ, Cao Y, Zhou G (2015) Prefabricated, ear-shaped cartilage tissue engineering by scaffold-free porcine chondrocyte membrane. Plast Reconstr Surg 135(2):313e–321e. doi:10.1097/PRS.0000000000001105

Liu Y, Zhang L, Zhou G, Li Q, Liu W, Yu Z, Luo X, Jiang T, Zhang W, Cao Y (2010) In vitro engineering of human ear-shaped cartilage assisted with CAD/CAM technology. Biomaterials 31(8):2176–2183. doi:10.1016/j.biomaterials.2009.11.080

Lopez-Lopez MT, Scionti G, Oliveira AC, Duran JD, Campos A, Alaminos M, Rodriguez IA (2015) Generation and characterization of novel magnetic field-responsive biomaterials. PLoS ONE 10(7):e0133878. doi:10.1371/journal.pone.0133878

Martinez-Outschoorn UE, Lin Z, Whitaker-Menezes D, Howell A, Lisanti MP, Sotgia F (2012) Ketone bodies and two-compartment tumor metabolism: stromal ketone production fuels mitochondrial biogenesis in epithelial cancer cells. Cell Cycle 11(21):3956–3963. doi:10.4161/cc.22136

Martin-Piedra MA, Garzon I, Oliveira AC, Alfonso-Rodriguez CA, Sanchez-Quevedo MC, Campos A, Alaminos M (2013) Average cell viability levels of human dental pulp stem cells: an accurate combinatorial index for quality control in tissue engineering. Cytotherapy 15(4):507–518. doi:10.1016/j.jcyt.2012.11.017

Martin-Piedra MA, Garzon I, Oliveira AC, Alfonso-Rodriguez CA, Carriel V, Scionti G, Alaminos M (2014) Cell viability and proliferation capability of long-term human dental pulp stem cell cultures. Cytotherapy 16(2):266–277. doi:10.1016/j.jcyt.2013.10.016

Matsumoto K, Kamiya N, Suwan K, Atsumi F, Shimizu K, Shinomura T, Yamada Y, Kimata K, Watanabe H (2006) Identification and characterization of versican/PG-M aggregates in cartilage. J Biol Chem 281(26):18257–18263. doi:10.1074/jbc.M510330200

Mills SE (2012) Histology for pathologists, 4th edn. Wolters Kluwer/Lippincott Williams & Wilkins Health, Philadelphia

Nayyer L, Patel KH, Esmaeili A, Rippel RA, Birchall M, O'Toole G, Butler PE, Seifalian AM (2012) Tissue engineering: revolution and challenge in auricular cartilage reconstruction. Plast Reconstr Surg 129(5):1123–1137. doi:10.1097/PRS.0b013e31824a2c1c

Oliveira JT, Reis RL (2011) Polysaccharide-based materials for cartilage tissue engineering applications. J Tissue Eng Regen Med 5(6):421–436. doi:10.1002/term.335

Oliveira JT, Crawford A, Mundy JM, Moreira AR, Gomes ME, Hatton PV, Reis RL (2007) A cartilage tissue engineering approach combining starch-polycaprolactone fibre mesh scaffolds with bovine articular chondrocytes. J Mater Sci Mater Med 18(2):295–302. doi:10.1007/s10856-006-0692-7

Oliveira AC, Garzon I, Ionescu AM, Carriel V, Cardona Jde L, Gonzalez-Andrades M, Perez Mdel M, Alaminos M, Campos A (2013) Evaluation of small intestine grafts decellularization methods for corneal tissue engineering. PLoS ONE 8(6):e66538. doi:10.1371/journal.pone.0066538

Pappa AK, Caballero M, Dennis RG, Skancke MD, Narayan RJ, Dahl JP, van Aalst JA (2014) Biochemical properties of tissue-engineered cartilage. J craniofac surg 25(1):111–115. doi:10.1097/SCS.0b013e3182a2eb56

Ren G, Crampton MS, Yap AS (2009) Cortactin: coordinating adhesion and the actin cytoskeleton at cellular protrusions. Cell Motil Cytoskeleton 66(10):865–873. doi:10.1002/cm.20380

Rodriguez MA, Lopez-Lopez MT, Duran JD, Alaminos M, Campos A, Rodriguez IA (2013) Cryopreservation of an artificial human oral mucosa stroma. A viability and rheological study. Cryobiology 67(3):355–362. doi:10.1016/j.cryobiol.2013.10.003

Rodriguez-Arco L, Rodriguez IA, Carriel V, Bonhome-Espinosa AB, Campos F, Kuzhir P, Duran JD, Lopez-Lopez MT (2016) Biocompatible magnetic core-shell nanocomposites for engineered magnetic tissues. Nanoscale 8(15):8138–8150. doi:10.1039/c6nr00224b

Roughley PJ (2006) The structure and function of cartilage proteoglycans. Eur Cell Mater 12:92–101

San Martin S, Alaminos M, Zorn TM, Sanchez-Quevedo MC, Garzon I, Rodriguez IA, Campos A (2013) The effects of fibrin and fibrin-agarose on the extracellular matrix profile of bioengineered oral mucosa. J Tissue Eng Regen Med 7(1):10–19. doi:10.1002/term.490

Scionti G, Moral M, Toledano M, Osorio R, Duran JD, Alaminos M, Campos A, Lopez-Lopez MT (2014) Effect of the hydration on the biomechanical properties in a fibrin-agarose tissue-like model. J Biomed Mater Res A 102(8):2573–2582. doi:10.1002/jbm.a.34929

Silva JM, Georgi N, Costa R, Sher P, Reis RL, Van Blitterswijk CA, Karperien M, Mano JF (2013) Nanostructured 3D constructs based on chitosan and chondroitin sulphate multilayers for cartilage tissue engineering. PLoS ONE 8(2):e55451. doi:10.1371/journal.pone.0055451

Tsai MC, Hung KC, Hung SC, Hsu SH (2015) Evaluation of biodegradable elastic scaffolds made of anionic polyurethane for cartilage tissue engineering. Colloids Surf B Biointerfaces 125:34–44. doi:10.1016/j.colsurfb.2014.11.003

Wight TN (2002) Versican: a versatile extracellular matrix proteoglycan in cell biology. Curr Opin Cell Biol 14(5):617–623

Wu JZ, Herzog W (2002) Elastic anisotropy of articular cartilage is associated with the microstructures of collagen fibers and chondrocytes. J Biomech 35(7):931–942

Yammani RR (2012) S100 proteins in cartilage: role in arthritis. Biochim Biophys Acta 1822(4):600–606. doi:10.1016/j.bbadis.2012.01.006

Yanaga H, Imai K, Koga M, Yanaga K (2012) Cell-engineered human elastic chondrocytes regenerate natural scaffold in vitro and neocartilage with neoperichondrium in the human body post-transplantation. Tissue Eng Part A 18(19–20):2020–2029. doi:10.1089/ten.TEA.2011.0370

Zhao X, Bichara DA, Zhou L, Kulig KM, Tseng A, Bowley CM, Vacanti JP, Pomerantseva I, Sundback CA, Randolph MA (2015) Conditions for seeding and promoting neo-auricular cartilage formation in a fibrous collagen scaffold. J Craniomaxillofac Surg 43(3):382–389. doi:10.1016/j.jcms.2014.12.007